Viable Synergy between Laboratory and Astrophysical Plasmas

G. Montani^{1,3}

¹ENEA, FSN Dept., C.R. Frascati, Via E. Fermi 45, 00044 Frascati, Italy ³Physics Dept., "Sapienza" University of Rome, P.le Aldo Moro 5, 00185 Roma, Italy

WiP - March 2nd 2020

Description

PLUS Collaboration: Plasma in Laboratory and Universe Systems.
 Promote Italian activities in Plasma Physics, especially with respect to cross-fertilization between Laboratory and Astrophysical scenarios.
 https://www.afs.enea.it/project/astro

 Research Lines: Acceleration in Plasmas; Accretion onto Compact Objects; Fusion and Diagnostic Devices; Self-Gravitating Systems.

Scientific Board:

- Elena Amato (INAF Arcetri Observatori (Florence))
- Stefano Atzeni (SBAI Dep., "Sapienza" Univ. of Rome)
- Marica Branchesi (GSSI, L'Aquila)
- Roberto Capuzzo Dolcetta (Physics Dep., "Sapienza" Univ. of Rome)
- Cristina Falvella (ASI)
- Massimo Ferrario (INFN, L.N. Frascati (Rome))
- Luigi Stella (INAF OAR, Monteporzio Catone (Rome))
- Marco Tavani (INAF IAPS, Rome)
- Angelo Tuccillo (CREATE)

Staff Members:

Coordinator: Giovanni Montani.

Franco Alladio (ENEA, Fusion and Nuclear Safety Department, C. R. Frascati (Rome)); Stefano Ascenzi (INAF-OA Brera, Milan): Roberto Bruno (INAF-IAPS, Rome): Paolo Buratti (ENEA, Fusion and Nuclear Safety Department, C. R. Frascati (Rome)); Nakia Carlevaro (ENEA, Fusion and Nuclear Safety Department, C. R. Frascati (Rome)); Sabrina Casanova (Max Planck, Heidelberg); Francesco Cianfrani (University of Marseille); Giuseppe Dattoli (ENEA, Fusion and Nuclear Safety Department, C. R. Frascati (Rome)); Matteo Del Prete (Physics Department, "Sapienza" University of Rome); Andrea Doria (ENEA, Fusion and Nuclear Safety Department, C. R. Frascati (Rome)); Matteo V. Falessi (ENEA, Fusion and Nuclear Safety Department, C. R. Frascati (Rome)); Alessandre Fassina (IGI, CNR); Marco Feroci (INAF-IAPS, Rome); Donatella Fiorucci (RFX Consotium, Padova); Lori Gabellieri (ENEA, Fusion and Nuclear Safety Department, C. R. Frascati (Rome)); Alfredo Luminari (PhD Student - Ast. Roma1 - Tor Vergata (Rome)); Fabio Moretti (Physics Department, "Sapienza" University of Rome); Roberto Onofrio (ENEA, Fusion and Nuclear Safety Department, C. R. Frascati (Rome)); Francesco Piacentini (Physics Department, "Sapienza" University of Rome); Fulvia Pucci (National Institute of Natural Science, Japan and Princeton University); Daniela Pugliese (University of Opava); Fabrizio Renzi (Physics Department, "Sapienza" University of Rome); Stefano Romeo (LNF -INFN); Raffaella Schneider (Physics Department, "Sapienza" University of Rome); Angelo Schiavi (SBAI Department, "Sapienza" University of Rome); Brunello Tirozzi (ENEA, Fusion and Nuclear Safety Department, C. R. Frascati (Rome)); Onofrio Tudisco (ENEA, Fusion and Nuclear Safety Department, C. R. Frascati (Rome)); Cristina Vaccarezza (INFN, L.N. Frascati (Rome)); Gregorio Vlad (ENEA, Fusion and Nuclear Safety Department, C. R. Frascati (Rome)); Angelo Vulpiani (Physics Department, "Sapienza" University of Rome); Fulvio Zonca (ENEA, Fusion and Nuclear Safety Department, C. R. Frascati (Rome); Institute for Fusion Theory and Simulation and Department of Physics, Zhejiang University, Hangzhou (China)).

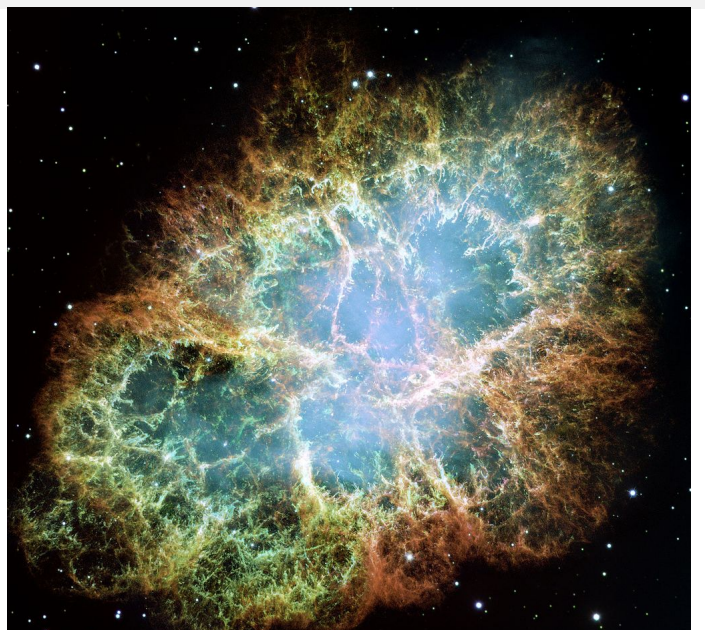
• Activities:

- Dedicated J. Plasma Phys. Thematic Issue (TBP in May 2020)
- Workshop PLUS. ENEA, C.R. Frascati November 06, 2019
- Meeting PLUS. Physics Department, "Sapienza" July 02, 2019
- Thematic workshop: Plasma acceleration.
 ENEA, C.R. Frascati May 13, 2019
- Mini-workshop. ENEA, C.R. Frascati March 05, 2019
- Workshop. ENEA, C.R. Frascati June 21, 2018
- Workshop. Physics Department, "Sapienza" October 23, 2018
- General meeting. ENEA, C.R. Frascati March 05, 2018
- Mini-workshop. ENEA, C.R. Frascati January 16, 2018

Selected Talks:

- Gian Piero Gallerano: Terahertz and mm-waves FEL applications at ENEA Frascati
- Roberto Capuzzo Dolcetta, Gravitational Dynamics in an extreme environment
- <u>Fulvia Pucci</u>, Energy transfer and electron energization in collisionless magnetic reconnection for different guide-field intensities
- Stefano Atzeni, Laser-driven inertial fusion and matter in stellar conditions
- <u>Franco Alladio</u>, Status of the art and operation plans of PROTO-Sfera
- Andrea Doria, Relativistic Electrons Based Radiation Sources
- G. Dattoli, Plasma accelerated e-beams and Free Electron Lasers?
- S. Ascenzi, Controparti elettromagnetiche di coalescenza di binarie compatte
- M. Feroci, Nuovi rivelatori per nuove diagnostiche in Astronomia X
- <u>F. Zonca</u>, Nonlinear wave-particle interaction in rising tone chorus generation
- M. Ferrario, Nuove Tecniche di Accelerazione ad EuPRAXIA@SPARC_LAB
- M. Tavani, La fisica di AGILE: nuovi scenari per l'emissione ad alte energie
- L. Stella, Magnetosfere di stelle di neutroni in accrescimento e di magnetar
- G. Vlad, Le prospettive della fusione italiana ed europea con DTT
- P. Buratti, Flares from the Crab Nebula

Crab Nebula



 Four intense gamma-ray flaring episodes from the Crab Nebula have been reported in the gamma-ray energy range 100MeV - a few GeV by AGILE and Fermi/LAT in the period 2007-2011.

[M. Tavani et al., Science 331, 736 or 739 (2011); V. Vittorini et al., ApJ 732, L22 (2011)]

- This activity has been attributed to transient emission in the inner Nebula due to the lack of:
 - any variation in the pulsed signal of the Crab pulsar;
 - any detectable alternative counterpart.
- High spatial resolution optical and X-ray obs. by Hubble Telescope and Chandra detected local enhancement in the "anvil" region.

[A. Tennant et al., ATel 2882, 1 (2010); P. Caraveo et al., ATel 2903,1 (2010)]

- The emission can be modelled as rapid (within 1day) acceleration followed by synchrotron cooling.
- Assuming a bulk Doppler factor ~ 1 and a local magnetic field $B_{loc} \sim 1 \text{mG}$, the energy for the synchrotron photons implies that the electrons are accelerated to $\gamma \sim 10^9$.

The striped pulsar wind:

- In the equatorial belt, the magnetic field at a fixed radius alternates in direction at the frequency of rotation, being connected to a different magnetic pole every half-period.
- The flow evolves into regions of magnetically-dominated cold plasma, separated by a very narrow, hot, corrugated surface (current sheet), whose amplitude increases linearly with the distance from the star.
- Wavelength of oscillations is at most $2\pi r_L$, where $r_L = cP/2\pi$ is the light cylinder radius and P the pulsar period (Crab: P = 33ms).
- The current sheet cuts the equatorial plane, and locally it resembles a sequence of concentric, spherical surfaces: striped wind.

[F.C. Michel, Comments Astro-phys. Space Phys. 3, 80 (1971)]

 Only some fraction of the magnetic energy can be converted into particle energy via a magnetic reconnection process in the wind before the termination shock.
 [Y. Lyubarsky, J.G. Kirk, ApJ 547, 437 (2001)]

Shock-driven reconnection and Crab flares:

- Lyubarsky analytical model for the particle acceleration via the shock-driven magnetic reconnection: [Y.E. Lyubarsky, Mon. Not. RAS 345, 153 (2003)]
 - Maximal Lorentz factor a particle can attain in the plasma comoving frame, when the magnetic field dissipates completely:

$$\gamma_{M} = \frac{1}{\Delta_{o}} \left[\frac{2-s}{2(s-1)} \sigma \right]^{1/(2-s)}$$

where $s \sim 1.5$ is the power-law index of particle distribution;

• maximal energy in the particle distribution in the laboratory frame:

$$\gamma_{\max} \sim \gamma_M \; \Gamma_w/k \sim \frac{\Gamma_w}{\Delta_o^{s-1}} \Big[\frac{2-s}{2(s-1)}\sigma\Big]^{1/(2-s)}$$

• For the **Crab Nebula** $\gamma_{max} \simeq 10^9 R_{15}^{-3/4}$. If a shock forms in a region well inside the termination shock and compresses the pulsar wind at 10^{15} cm from the inner pulsar, this calculation shows that high energy electrons can be accelerated up to $\gamma_{max} \simeq 10^9$ in the laboratory frame.

A collisionless shock compressing the pulsar wind:

- Assume that a shell of overdense material of total energy E_o is created in the vicinity of the central pulsar, composed by photon and e^{\pm} pairs, and loaded with baryons: **fireball model**. [T. Piran, Phys. Rept. 333, 529 (2000)]
- Issues against this formulation:
 - Fireball acceleration Γ_f is highly relativistic, at least one order of magni- tude larger than Γ_w at $10^{15} \mathrm{cm}$: the initial shell is *radiation dominated*. Thus, most of the fireball energy content is radiated as thermal emission when the fireball becomes transparent, at $T_{obs} = \Gamma_f \times 20 \mathrm{keV} \sim 100 \mathrm{MeV}$. It should have been detected by a gamma-ray instrument;
 - in an almost pure radiation fireball, the transparency is reached too early to accelerate the baryons to such a high Lorentz factor;
 - alternative possibility: the fireball is highly magnetized (acceleration driven by magnetic pressure instead of radiation pressure). But the baryon acceleration is even less efficient, scaling as $\Gamma \propto r^{1/3}$.

A plasma instability?

- Required properties of a plasma instability:
 - the shock-induced magnetic reconnection requires necessarily a supersonic compression of particles and of magnetic field characterizing the wind;
 - the wind is strongly dominated by the magnetic energy and the Alfvén velocity is supersonic in the medium.
- We propose the Weibel instability: anisotropy of the wind temperature.
 [E.S. Weibel, Phys. Rev. Lett. 2, 83 (1959)]
- Since the compression of the sheet is radial, we can infer a radial propagation of the instability, associated with a different radial temperature of the wind with respect to the orthogonal one.

Pulsar wind equilibrium distribution function:

$$f_0 = \frac{n}{u_p^2 u(2\pi)^{3/2}} \exp\left[\frac{v_p^2}{2u_p^2} + \frac{v^2}{2u^2}\right]$$

 (v_p, u_p) and (v, u) are the particle velocity and its variance on a given plane and in the orthogonal direction. n the wind particle density.

• Growth rate for $u_p \gg u$:

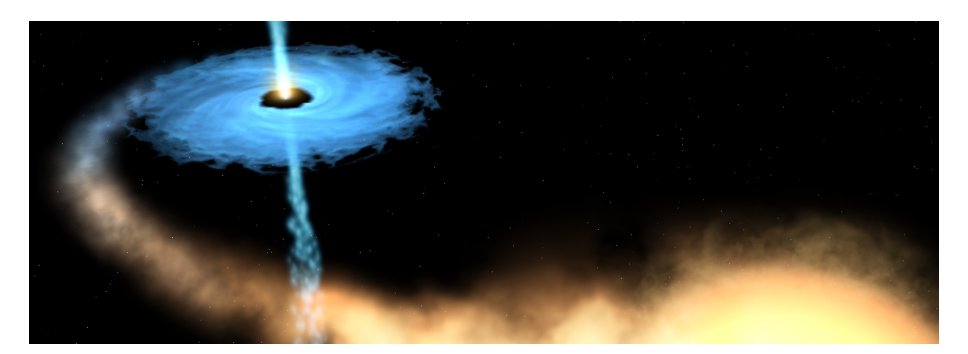
$$\gamma(k) = k u_p \omega_p / \sqrt{\omega_p^2 + c^2 k^2}$$

• At $r\simeq 10^{15} {\rm cm}$: $n\simeq 10^{-3} {\rm cm}^{-3}$, $\omega_p\simeq 10^3 {\rm s}^{-1}$. Furthermore, $\omega_p\gg c/\lambda_s$ (where $\lambda_s\gg\lambda_D\simeq 10^7 {\rm cm}$ is sheet scale). Thus, on the sheet scale,

$$\gamma \simeq 10\,\mathrm{s}^{-1}$$

• The Crab wind is collisionless: anisotropy must come from the pair e^{\pm} generation mechanism.

Accretion in Astrophysics



Axisymmetric thin disk model

Accretion disk configuration around a central object.

- stationary configuration

- compact: $M_{\rm S} \sim 1.5 - 2 M_{\odot}$

Features

 $R_{\rm S} \sim R_{\rm Sch} = 2 G M_{\rm S}/c^2$ - strongly magnetized: $B \sim 10^{12}-10^{14} {\rm G}$

Thin disk condition: $H_0(r)/r \ll 1$

Newton potential:
$$\chi(r,z) = -\frac{GM_{\rm S}}{\sqrt{r^2+z^2}}$$

Axisymmetric Field:
$$\vec{B} = -\frac{1}{r}\partial_z\psi\vec{e}_r + \frac{I}{r}\vec{e}_\phi + \frac{1}{r}\partial_r\psi\vec{e}_z$$

Dipole Field approximation:
$$\psi_{\rm D} = \frac{\mu_0 r^2}{(r^2 + z^2)^{3/2}}$$

Corotation theorem:
$$\omega = \omega(\psi)$$

 $\rightarrow H_0$: half depth of the disk.

Fluid Dynamics

- Radial Eq:
$$\rho_0 v_r \frac{\partial v_r}{\partial r} - \rho_0 \left(\omega^2 r - \frac{\partial \chi}{\partial r} \right) + \frac{\partial p}{\partial r} = 0$$

- Vertical Eq:
$$\frac{\partial p}{\partial z} = -\rho \frac{\partial \chi}{\partial z}$$

- Azimuthal Eq:
$$\frac{\dot{M}}{2\pi r}\frac{\partial j}{\partial r} = \frac{2}{3}\alpha\frac{\partial}{\partial r}\left(\Sigma v_{\rm S0}H_{0}r^{3}\frac{\partial\omega}{\partial r}\right)$$

- Continuity Eq:
$$\frac{\partial \dot{M}}{\partial r} = 0$$

Definitions:

$$\Sigma = \int_{-z_0}^{z_0} \rho dz \qquad \dot{M} = -2\pi r \Sigma v_r \qquad j = r v_\phi$$
$$\rho_0 = \rho(z = 0) \qquad \omega = \frac{v_\phi}{r}$$

[G.S. Bisnovatyi-Kogan, R.V.E. Lovelace, New. Astro. Rev. 45, 663 (2001)]

In the case of a polytropic equation of state

$$p = \kappa \rho^{1+1/\gamma}$$

from the vertical equation we have that

$$\rho = \rho_0 \left(1 - \frac{z^2}{H_0^2} \right)^{\gamma} = \left[\frac{GM_{\text{S}}}{2\kappa \left(\gamma + 1 \right)} \right]^{\gamma} \left(1 - \frac{z^2}{H_0^2} \right)^{\gamma}$$

Isothermal case: $p = \kappa \rho$

$$\rho = \rho_0 \exp\left(-\frac{z^2}{H_0^2}\right) \qquad H_0 = \left(\frac{2\kappa r^3}{GM_S}\right)^{1/2}$$
$$\Sigma = \left(\frac{2\pi\kappa}{GM_S}\right) \rho_0 r^{3/2} \qquad v_{s0} = \sqrt{\kappa}$$

$$\omega \simeq \omega_{\mathsf{K}} = \sqrt{\frac{GM_{\mathsf{S}}}{r^3}}$$

From the azimuthal eq, introducing the coefficient α ,

$$\frac{\dot{M}}{2\pi}(j-j_0) = \frac{2}{3}\alpha \Sigma v_{s0} H_0 r^3 \frac{\partial \omega}{\partial r}$$

Positive value of j_0 corresponds to a negative total flux \Rightarrow The central body accretes its total angular momentum.

Ngative value of j_0 corresponds to a mass increase \Rightarrow Te central body decreases its total angular momentum.

Shakura Standard Model and its issues

The inward matter flux is due to viscous stresses.

The coefficient α scales the viscosity coefficient η_v :

$$\eta_v = \frac{2}{3}\alpha\rho v_{s0}H_0 \iff \dot{M} = 4\pi\alpha\rho v_{s0}H_0^2 \iff \tau_{r\phi} = -\alpha\rho v_{s0}^2$$

Turbulent enhancement: a non-vanishing viscosity exists in quasi-ideal astrophysical plasmas, but the Shakura paradigm hides in α every *effective* treatment needed to reach the observed accretion rate.

Let $\xi < 1$ be an efficiency such that the luminosity $\mathcal{L}_{acc} = \xi \mathcal{L}_{Edd}$:

$$\frac{GM_{\rm S}\dot{M}_{\alpha}}{R_{\rm S}} = \xi \frac{GM_{\rm S}m_pc}{\sigma_{\rm Th}} \implies \alpha_{\rm Sh} = \xi \frac{c}{v_{\rm s0}} \frac{R_{\rm S}\,\ell_{\rm Th}}{H_0}$$

where σ_{Th} is the Thomson cross-section. The microscopical viscosity due to ion-ion collisions is estimated as:

$$\eta_v = \frac{\rho v_{s0}^2}{\nu_{ii}} \implies \alpha_{id} = \frac{3}{2} \frac{\ell_{ii}}{H_0}$$

The *effective* parametrization accounts for several orders of magnitude with respect to microscopical conditions:

$$\frac{\alpha_{\rm Sh}}{\alpha_{\rm id}} = \frac{2}{3} \xi \frac{c}{v_{\rm s0}} \frac{R_{\rm S}}{H_0} \frac{\ell_{\rm Th}}{\ell_{\rm ii}} \simeq 10^{-3} \cdot 10^3 \cdot 10^{-2} \cdot 10^{10} = 10^8$$

Towards an alternative paradigm

Generalized Ohm Law: background \vec{B}_0 and backreaction \vec{B}_1

$$ec{E}_{\phi} + rac{1}{c} (ec{v} imes ec{B})_{\phi} = ec{J_{\phi}}/\sigma \quad \Longrightarrow \quad v_r B_0 \simeq rac{c^2}{4\pi\sigma} rac{B_1}{\lambda}$$

 λ is the backreaction length-scale, responsible for the induced currents.

The **Magnetic Prandtl Number**: since v_r depends on radius r and viscosity η_v , we can derive:

$$\mathsf{PrM}(n_e,T) \equiv rac{4\pi\sigma\eta_v}{
ho c^2} pprox rac{r}{\lambda} rac{B_1}{B_0}$$

It can be shown that $PrM \gg 1$ in typical disk ranges

- $10^8 \lesssim n_e \lesssim 10^{12} \mathrm{cm}^{-3}$
- $10^5 \lesssim T \lesssim 10^8 \text{K}$

In the Standard Model, $B_1 \ll B_0$ and $\lambda \simeq r \simeq R_{\rm disk}$: effective small PrM with a surprisingly small effective conductivity.

For reasonable $B_1 \lesssim B_0$, the huge values of realistic (i.e., non-effective) PrM ask for the formation of **microstructures** with $\lambda \ll r \simeq R_{\rm disk}$.

[G. Montani, J. Petitta, Phys. Rev. E 87, 053111 (2013)]

Local Formulation

- We choose a fixed value $r=r_0$
- Isothermal condition
- Hierarchy ordering of the gradients

$$\psi = \psi_0 + \psi_1 \quad (\psi_1 \ll \psi_0)$$

$$\omega \simeq \omega_K + \delta \omega \simeq \omega_K + \psi_1 d\omega/d\psi_0$$

$$\rho = \bar{\rho}(r_0, z^2) + \hat{\rho}(r_0, z^2, r - r_0)$$

$$p = \bar{p}(r_0, z^2) + \hat{p}(r_0, z^2, r - r_0)$$

Vertical Configuration
$$\begin{cases} D(z^2) \equiv \frac{\epsilon}{\rho_0(r)} \\ \rho_0(r_0) \equiv \rho(r_0) \end{cases}$$

$$\begin{aligned} & \text{Vertical} \\ & \text{Configuration} \end{aligned} \begin{cases} D(z^2) \equiv \frac{\bar{\rho}}{\rho_0(r_0)} = \exp\left(-\frac{z^2}{H_0^2}\right) \\ & \rho_0(r_0) \equiv \rho(r_0, \, 0) \,, \, H_0^2 \equiv \frac{4K_B\bar{T}}{m_i\omega_K^2} \\ & \partial_z \hat{p} + \omega_K^2 z \hat{\rho} + \frac{1}{4\pi r_0^2} \left(\partial_z^2 \psi_1 + \partial_r^2 \psi_1\right) \partial_z \psi_1 = 0 \end{cases}$$

$$\begin{array}{l} \text{Radial} \\ \text{Configuration} \end{array} \begin{cases} \omega \simeq \omega_{\text{K}} + \delta \omega \simeq \omega_{0}(\psi_{0}) + \omega_{0}' \psi_{1} \\ 2\omega_{\text{K}} r_{0}(\bar{\rho} + \hat{\rho}) \omega_{0}' \psi_{1} + \frac{1}{4\pi r_{0}^{2}} \left(\partial_{z}^{2} \psi_{1} + \partial_{r}^{2} \psi_{1}\right) \partial_{r_{0}} \psi_{0} = \\ = \partial_{r} \left[\hat{p} + \frac{1}{8\pi r_{0}^{2}} \left(\partial_{r} \psi_{1}\right)^{2} \right] + \frac{1}{4\pi r_{0}^{2}} \partial_{r} \psi_{1} \partial_{z}^{2} \psi_{1} \end{cases}$$

[B. Coppi, Phys. Plasmas 12, 057302 (2005)]

19/28

Astrophysical Jets

Relativistic jets are features that the more extreme AGNs and XRBs have in common. It is usually inferred that the basic physics must be the same, with peculiarities due only to the different scales.

AGNs, XRBs, Supernovae, GRBs:

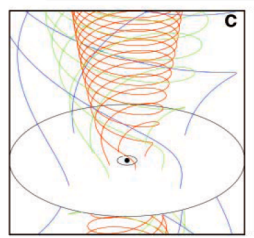
In all observed cases the central object is compact, either a NS or a BH, and is accreting matter and angular momentum. In most systems there is evidence of magnetic fields (detected in the synchrotron radiation or inferred in collapsing supernovae cores from SNRs). The combination of magnetic fields and rotation is hold responsible for the observed relativistic jets.

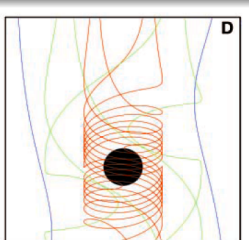
AGN case

AGN jets can flow at Lorentz factors \sim 50 and carry a highly energized plasma with a power greater than $10^{46} \,\mathrm{erg}\,\mathrm{s}^{-1}$. The central engine is an accreting SMBH with a mass in $10^6 - 10^{10} M_{\odot}$. The accretion disk emits thermal ultraviolet, optical, and infrared radiation. There must also be a corona of hot electrons that Compton-scatters photons to X-ray energies.

The current picture of jet formation invokes differential rotation of the poloidal component of the magnetic field either in the inner disk or in the BH ergosphere, neither fully satisfying:

- Accelerating a disk-propelled jet to ultrarelativistic flow speeds is hard because of the diffusive nature of the magnetic field in the accepted Shakura Model;
- ▶ Jets launched from the ergosphere can reach high Lorentz factors provided a high initial energy-to-matter ratio (but it works only on rotating SMBHs).



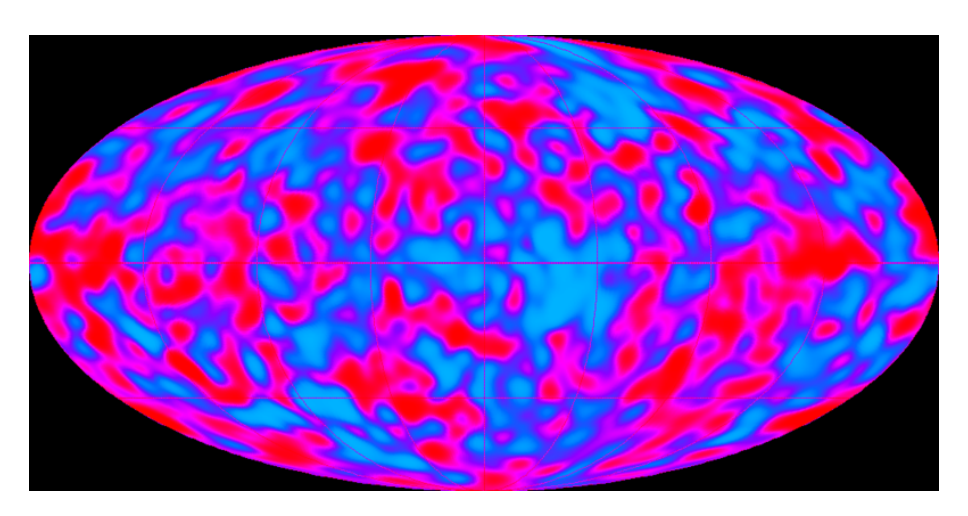


Schematic diagrams of jet-triggering scenarios, adapted from [1].

- (C) The poloidal magnetic field of a disk will bring coronal plasma outward in a wind; if the outblow has enough energy density, it can sweep back and coil the field lines.
- (D) The dragging of inertial frames near a rotating BH forces the plasma to co-rotate inside the ergosphere; the field lines will be drawn inward (only the vertical component is shown in figure).

[1] Meier et al. (2001): Science 291, 84.

Cosmological Plasma



Between the e^+e^- annihilation ($T=T_{e^+e^-}\simeq 1\,\mathrm{MeV}\simeq 2\times 10^{10}\,\mathrm{K}$) and the hydrogen recombination ($T=T_{\mathrm{rec}}\simeq 0.25\,\mathrm{eV}\simeq 3000\,\mathrm{K}$), the cosmological fluid is a plasma of electrons, protons and photons.

ightarrow Baryon-to-photon ratio is extremely small: $\eta_B \equiv n_B/n_\gamma \simeq 6 \times 10^{-10}$ Both n_B and n_γ evolve as: $n_{B,\gamma}(z) = n_{B,\gamma}^0(1+z)^3$ Today we have: $n_B^0 \simeq 2.5 \times 10^{-7} \, {\rm cm}^{-3}$ and $n_\gamma^0 \simeq 410 \, {\rm cm}^{-3}$ (z: redshift, n_γ : photon number density, n_B : the sum of the proton n_P and of the neutron n_N number densities, superscript 0 : present value of a quantity.)

Because of the smallness of the helium-to-hydrogen ratio ($\simeq 1/10$), we assume $n_B=n_p=n_e$ because of the charge neutrality of the Universe. (n_e being the electron number density)

Since
$$T(z) = T^0(1+z)$$
, the **Debye length** $\lambda_D = \sqrt{T/4\pi n_e e^2}$ results

$$\lambda_D(z) = \frac{2.3 \times 10^4 \, \text{cm}}{1 + z}$$

Plasma parameter N_D (the number of particles within a Debye sphere)

$$N_D = \frac{4\pi}{3} n_p \lambda_D^3 \simeq 10^7 \gg 1$$

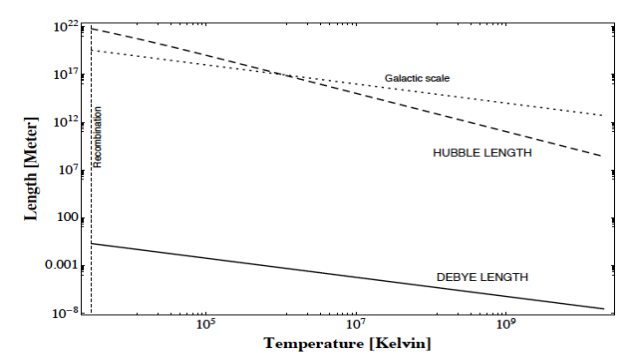
It results that the cosmological fluid is a weakly coupled plasma.

The comoving Debye length $\bar{\lambda}_D \equiv \lambda_D(1+z)$ is constant during the Universe evolution and equal to $\bar{\lambda}_D \simeq 2 \times 10^4 \, \mathrm{cm}$.

 \rightarrow The (physical) Debye length has to be compared with the *physical length* of the Universe, given by the Hubble length $l_H = cH^{-1}$.

Today: $l_H^0 \simeq 10^{28}\,{\rm cm};$ matter-dominated era: $l_H \propto (1+z)^{-3/2};$ radiation-dominated era: $l_H \propto (1+z)^{-2}.$

Plot: Evolution of the Debye length $\lambda_D \propto T^{-1}$ and of the Hubble length $l_H \propto T^{-3/2}$.



 l_H ≫ λ_D: The cosmological fluid can be considered as neutral at all scales of cosmological interest. For an electron-proton plasma, plasma resistivity η is given by

$$\eta = \frac{m_e \nu_{ei}}{n_e e^2}$$

 $(m_e$: electron mass, ν_{ei} : electron-ion-collision frequency)

 $\rightarrow \nu_{ei}$ is approximated by the electron-electron collision frequency ν_{ee}

$$v_{ei} \simeq v_{ee} \simeq 2.91 \times 10^{-6} \, {
m sec}^{-1} \left(rac{n_e}{{
m cm}^{-3}}
ight) \left(rac{T}{{
m eV}}
ight)^{-3/2} \ln \Lambda$$

 $ln \Lambda$: Coulomb logarithm

(quantify the effects of small-angle-diffusion collisions in the Coulomb scattering.)

A simple estimate of Λ in a plasma is given by $\Lambda \simeq 12\pi N_D$, so that for the cosmological fluid, the Coulomb logarithm is $\simeq 20$.

Finally we get

$$\eta(z) \simeq 1.6 imes \left(rac{1+z}{1100}
ight)^{-3/2} {
m Ohm~cm}$$

Near recombination, the cosmological plasma has an electric resistivity

$$\eta \simeq 1.6 \, \text{Ohm cm}$$

i.e., a conductivity $\simeq 0.6$ S cm $^{-1}$, a value typical of a semiconductor.

Selected Articles

- G. Montani e R. Benini, "Linear 2-dimensional MHD of Accretion disks: Crystalline structure and radial matter infall", Mod. Phys. Lett. A, 24, 2667 (2009).
- M. Lattanzi, G. Montani, "A Separable Solution for the Oscillatory Structure of Plasma in Accretion Disks", Europhys. Lett. 89, 39001 (2010).
- G. Montani, N. Carlevaro, "High Peaks in the Axial Velocity for an Ideal MHD disk Configuration", Phys. Rev. E 82, 025402(R) (2010).
- G. Montani, R. Benini, "Viscoresistive MHD configurations of plasma in accretion disks", Gen. Rel. Grav. 43, 1121 (2011).
- G. Montani, R. Benini, "Crystalline structure of accretion disks: features of a global model", Phys. Rev. E 84, 026406 (2011).
- R. Benini, G. Montani, J. Petitta, "Ring sequence decomposition of an accretion disk: the viscoresistive approach", Europhys. Lett. 96, 19002 (2011).
- D. Pugliese, N. Carlevaro, M. Lattanzi, G. Montani, R. Benini, "Stability of a self-gravitating homogeneous resistive plasma", *Physica D* 241, 721 (2012).
- M. Lattanzi, N. Carlevaro, G. Montani, "Gravitational instability of the primordial plasma: anisotropic evolution of structure seeds", Phys. Lett. B 718, 255 (2012).

- D. Pugliese, G. Montani, M.G. Bernardini, "On the Polish doughnut accretion disk via the effective potential approach", Mon. Not. RAS 428, 952 (2012).
- G. Montani, N. Carlevaro, "Inconsistency in the standard model for stellar thin accretion disks", *Phys. Rev. D* **86**, 123004 (2012).
- D. Pugliese, G. Montani, "Squeezing of toroidal accretion disks", Europhys. Lett. 101, 19001 (2013).
- G. Montani, J. Petitta, "Nonstationary magnetic microstructures in stellar thin accretion disks", *Phys. Rev. E* **87**, 053111 (2013).
- G. Montani, D. Pugliese, "Counterexample of the magneto-rotational instability in two-dimensional axial symmetry", *Phys. Rev. E* **88**, 033101 (2013).
- G. Montani, R. Benini, N. Carlevaro, A. Franco, "Thermomagnetic instability of a rotating magnetized plasma disk", Mon. Not. RAS 436, 327 (2013).
- G. Tirabassi, G. Montani, N. Carlevaro, "Self-collimated axial jets from thin accretion disks", Phys. Rev. E 88, 043101 (2013).
- G. Montani, J. Petitta, "Plasma phenomenology in astrophysical systems: radio-sources and jets", *Phys. of Plasmas* **21**, 061502 (2014).
- G. Montani, M.G. Bernardini, "The Crab Nebula flaring activity", Phys. Lett. B 739, 433 (2014).

- D. Pugliese, G. Montani, "Relativistic thick accretion disks: Morphology and evolutionary parameters", Phys. Rev. D 91, 083011 (2015).
- G. Montani, D. Pugliese, "Morphology of the two-dimensional MRI in Axial Symmetry", J. Plasma Phys. 81, 495810604 (2015).
- G. Montani, F. Cianfrani, D. Pugliese, "Implications of the Co-rotation Theorem on the MRI in Axial Symmetry", Astroph. J. 827, 24 (2016).
- N. Carlevaro, G. Montani, F. Renzi, "Study of MRI in stratified viscous plasma configuration", Europhys. Lett. 117, 49001 (2017).
- F. Cianfrani, G. Montani, "Revised conditions for MRI due to isorotation theorem", *Phys. Lett. B* **769**, 328 (2017).
- G. Montani, M. Rizzo, N. Carlevaro, "On the behavior of a thin disk crystalline morphology in presence of corrections to MHD", Phys. Rev. E 97, 023205 (2018).
- G. Montani, D. Pugliese, "Influence of toroidal magnetic field in multiaccreting tori", Mon. Not. RAS 476, 4346 (2018).
- G. Montani, G. Palermo, N. Carlevaro, "Coexistence of magneto-rotational and Jeans instabilities in an axisymmetric nebula", A&A 617, A112 (2018).